Low-Profile Omnidirectionally Radiated Microstrip Antenna for LEO Satellite Swarm Communication

Seongmin Pyo
Department of Information and Communication Engineering
Hanbat National University
Daejeon 34158, Rep. of Korea
spyo@edu.hanbat.ac.kr

Dongho Lee
epartment of Electrical and Control Engineering
Mokpo National University
Jeollanam-do 58554, Rep. of Korea
dongho.lee864@gmail.com

***Abstract*—This paper proposes a monopolar microstrip antenna with symmetric ring-shaped trapezoid ground slots. The center patch facilitates gap-coupling feeding directly connected with 50 Ohm coaxial line, while six gap-coupled radiators arranged in quasi-circle configuration. The trapezoid ground-slots beneath the six radiators serve to adjust the impedance bandwidth and reduce the overall antenna size. The proposed antenna exhibits omni-directional radiation pattern with broad bandwidth. From the optimization, we have obtained a smaller size and a thinner substrate of the proposed antenna.**

Keywords— hexagonal patch, omni-directional radiation, trapezoid ground slots, resonance modes.

I. Introduction

Monopole antennas are widely employed in wireless communication systems due to their ability to produce an omnidirectional radiation pattern and vertical polarization [1]. Unfortunately, a monopole antenna exhibits a disadvantage as it contributes to an elevated surface drag when mounted perpendicular to the ground surface on a rapidly moving vehicle. For this reason, the monopolar microstrip antenna was introduced in 1994 [5]. Since then, various iterations of monopolar microstrip antennas have been presented based on the design method of a center-fed structure with different resonant modes [6-10].

In this study, we introduce a monopolar microstrip antenna with quasi-circularly arranged hexagonal patches on the top of the substrate and the symmetric ring-shaped trapezoid ground slots. In addition, we focused the analyze and optimize the monopolar microstrip antenna with wide bandwidth based on the parametric studies. The following sections provide details regarding the proposed antenna configuration, reflection coefficient, radiation pattern, fractional bandwidth and the electric field distribution for operational principles.

II. Antenna Design and Configuration

A. Configuration

Fig. 1 illustrates the configuration of the proposed antenna, consisting of seven hexagonal patches on the top plane of the substrate. The center patch is connected to a 50 Ohm coaxial feed for gap-coupling feeding, while the remaining six patches function as radiators. The first yielding mode is identified as the non-fundamental 1.5 wavelength TM02 mode with omni-directional radiation pattern, attributed to the arrangement of the six radiators in a quasi-circle.

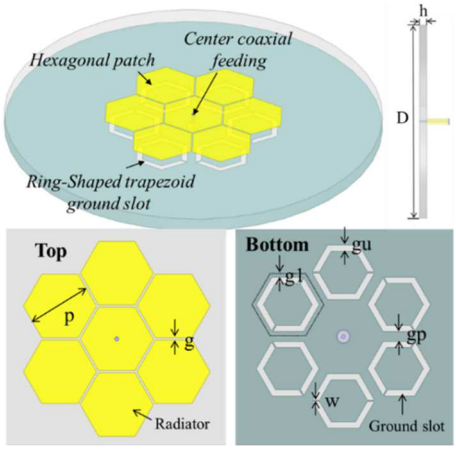

Fig. 1. Configuration of the proposed antenna.

Each of the six radiators equipped with ring-shaped symmetric trapezoid slots on the ground, strategically employed to adjust the impedance matching and bandwidth. Moreover, the significant change in the guided wavelength of the proposed antenna contributes to an overall reduction in antenna diameter. The antenna is designed on a 1.575 mm thick Roger RT/Duroid 5880 substrate with a dielectric constant of 2.2 and a loss tangent of 0.001. The antenna's diameter is set at 52 mm, and the individual length of each patch is 10 mm. To adhere to fabrication constraints, a 0.2 mm gap between each patch is chosen, and other dimensions on the ground plane are specified accordingly. Detailed final parameters are provided in Table 1.

TABLE I. Optimized Dimensions of The Proposed Antenna

Parameters	Symbol	Value(mm)
Patch length	p	10
Gap between patches	g	0.2
GND slot width	gu	1.8
GND wire width	w	0.2
GND space between 2 slots	gp	0.8
Distance between patch and slot edge	gl	0.3
Substrate diameter	D	52
Substrate thickness	h	1.575

B. *Operation Principle and Field Distribution*

To realize the operation principle of proposed antenna, equivalent magnetic current density, as shown in Fig 2. The traditional method to achieve the omni-directional radiation in microstrip antennas involves utilizing the equivalent magnetic loop current density of the radiator edge side, which is mathematically equal to the electric line current density. The magnetic loop currents along each radiating edge, situated along the periphery or perimeter of the resonator structure, are mathematically expressed as follows:

$$M_s = -2\hat{n} \times E \qquad (1)$$

where $\hat{n}$ and E are the normal unit vector toward the edge and E-filed at the edge, respectively.

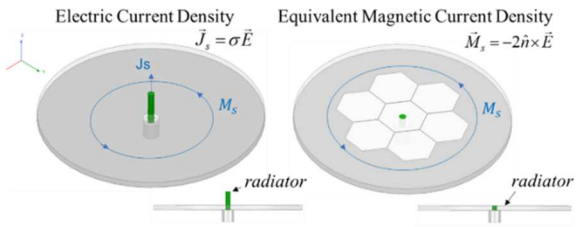

Fig. 2. Illustration of proposed antenna equivalent model.

Fig. 3 displays simulated electric field distributions at two adjacent resonant frequencies of proposed antenna. The result in Figs. 3(a) and 3(b), is indicating the successful resonance frequency at 5.61 GHz and 6.09 GHz. The simulated frequency responses of the proposed antenna, both with and without ground slots, are shown in Fig. 4. The results demonstrate that the absence of slots on the ground plane would originally result in around 9 GHz. However, upon the addition of the ring-shaped trapezoid ground slots, this frequency shifts to 5.61 GHz.

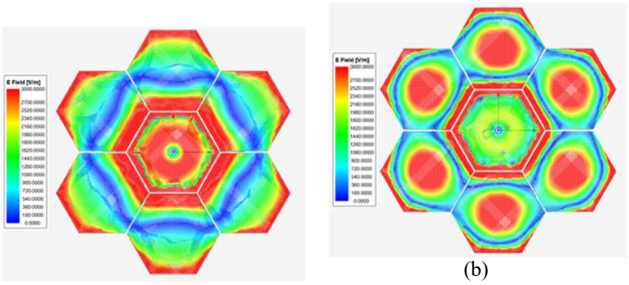

Fig. 3. Simulated electric field distributions (a) at 5.61 GHz and (b) at 6.09 GHz.

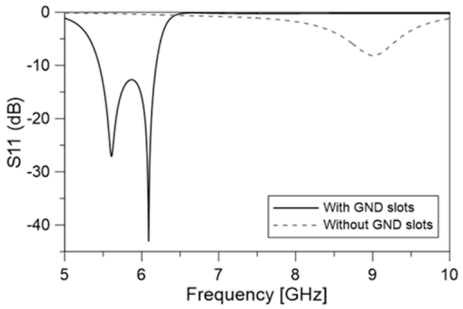

Fig. 4. Simulated reflection coefficient of proposed antenna with and without ground slots

C. *Parametric Analysis*

The parametric study of the frequency response variations for different parameters of the proposed antenna is presented in Fig. 5. All dimensions have been chosen to achieve broad bandwidth. The antenna design dimension are as follows: substrate thickness (h) = 1.575 mm, slot width (gu) = 1.8 mm, and substrate diameter (D) = 52 mm and distance between slot edges (gp) = 0.8 mm.

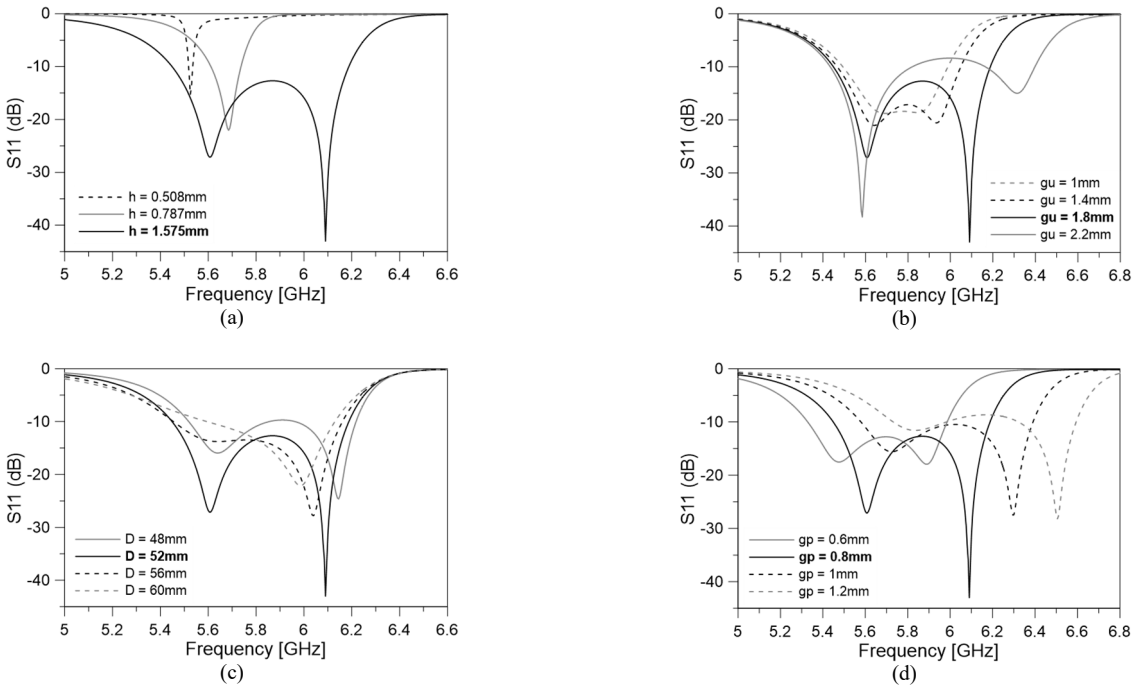

Fig. 5. The reflection coefficient results of parametric variation for proposed antenna (a) substrate thickness, (b) slot width, (c) diameter, and (d) dist. between two units of slots.

The substrate thickness is examined at standard values of 0.508 mm, 0.787mm, and 1.575 mm, maintaining a dielectric constant of 2.2. Results in Fig. 5(a) indicate that one of the resonant modes does not occur when the substrate thickness is decreased to 0.508 mm and 0.787 mm. Both resonant are strongly coupled with a broad bandwidth in the case in of h = 1.575 mm. Fig. 5(b), the graph depicts the influence of varying slot width on the proposed antenna. Reducing the slot width brings the two resonant frequencies closer, resulting in a bandwidth reduction. Conversely, a substantial increase in this slot width causes the two resonances to move apart, leading to poor impedance matching at center frequency. This underscores the slot width have critical role in the antenna's performance optimization. Fig. 5(c) illustrates the effect of diameter change on the reflection coefficient of the proposed antenna. The graph shows expected results, when the diameter was changed, dual resonant coupling varied. The higher resonant mode is maintained at around 5.9 GHz to 6.2 GHz, and the lower resonant frequency exhibits different coupling factors.

III. Implementation and Results

The physical dimensions of the proposed antenna were fine-tuned and are detailed in Table 1. The optimization process aimed to maximize the operating bandwidth while maintaining a low profile and achieving optimum frequency responses.

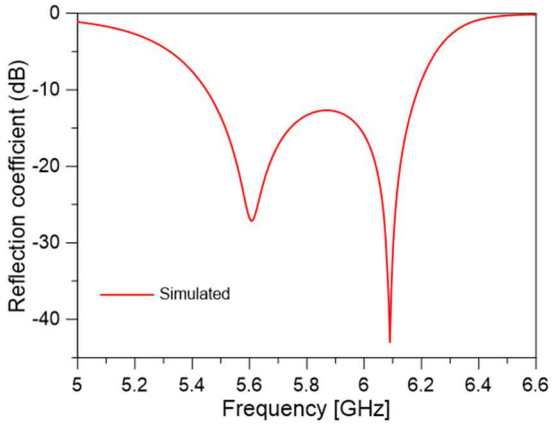

Fig. 6. Reflection coefficient of proposed antenna.

Fig. 6 displays the simulated reflection coefficients of the proposed antenna. The simulation result showed 10-dB impedance bandwidths of 760 MHz from 5.44 GHz to 6.2 GHz with respect to 13% fractional bandwidth.

Fig. 7 presents the far-field radiation patterns of the proposed antenna at 5.61 GHz and 6.09 GHz. The proposed antenna successfully demonstrated a robust omni-directional radiation pattern in both resonant frequencies. The peak gain is observed at $\theta = 36^{\circ}$ shown in Fig. 7(b) and (d).

The simulated antenna gains of the proposed design are displayed in Fig. 8. The realized gains consistently surpass 3 dBi across the frequency range from 5.4 GHz to 6.2 GHz. The peak gain is reaching 4.1 dBi at 5.61 GHz and 4 dBi at 6.09 GHz.

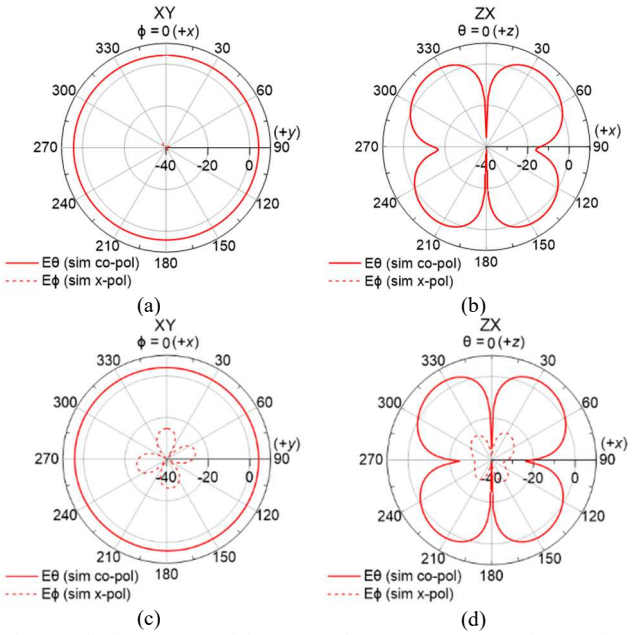

Fig. 7. radiation patterns of the proposed antenna at resonant frequencies above at 5.61 GHz and below at 6.09 GHz (a)(c) *H*-plane (xy-plane) and (b)(d) *E*-plane (zx-plane)

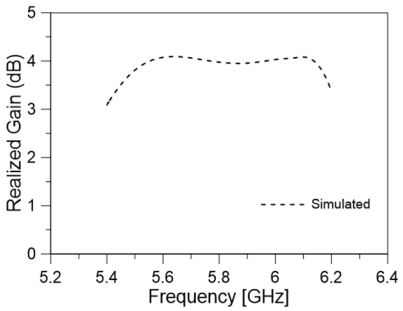

Fig. 8. Realized gain of proposed antenna.

IV. Conclusion

In this study, seven hexagonal patched monopolar microstrip antenna with a new symmetric ring-shaped trapezoid ground slots designed and introduced. Thanks to the significant impact of the symmetric ring-shaped trapezoid ground slots on the guided wavelength, the proposed antenna achieves an ultra-low profile with increased bandwidth and a favorable omni-directional radiation pattern across all operating bands. Therefore, the proposed antenna holds promise for future wireless communication applications.

Acknowledgement

This work was supported by Korea Research Institute for defense Technology planning and advancement (KRIT) grant funded by the Korea government (Defense Acquisition Program Administration, 21-106-A00-007) and also supported by the National Research Foundation of Korea(NRF) grant funded by the Korea government(MSIT) (No. 2022R1G1A1010219)

REFERENCES

[1] W. L. Stutzman and G. A. Thiele, Antenna Theory and Design, 2nd ed. New York, NY: Wiley, 1998.

[2] K. G. Thomas and N. Lenin, "Ultra-Wideband Printed Monopole Antenna," Microwave and Optical Technology Letter, vol. 49, no. 5, pp. 1082-1085, 2007.

[3] A. Iqbal, A. Smida, N. Mallat, M. Islam, and S. Kim, "A Compact UWB Antenna with Independently Controllable Notch Bands," MDPI Sensors, vol. 19, no. 6, pp. 1411, 2019.

[4] S. Ahmad, U. Ijaz, and S. Naseer, "A Jug-Shaped CPW-Fed Ultra-Wideband Printed Monopole Antenna for Wireless Communications Networks," MDPI Applied Sciences, vol. 12, no. 2, pp. 821, 2022.

[5] B. A. Burberry and P. R. Foster, "New Kind of Microstrip Antenna: The Monopolar Wire Patch Antenna," Electronics Letters, vol. 30, no. 10, pp. 745, 1994.

[6] J. Liu, Q. Xue, H. Wong, and Y. Long, "Design and Analysis of a Low-Profile and Broadband Microstrip Monopolar Patch Antenna," IEEE Transactions on Antennas and Propagation, vol. 61, no. 1, pp. 11-18, 2013.

[7] X. Q. Zhu, Y. X. Guo, and W. Wu, "A Novel Dual-Band Antenna for Wireless Communication Applications," IEEE Antennas and Wireless Propagation Letters, vol. 15, pp. 516–519, 2016.

[8] S. Wang, L. Zhu, J. Wang, and W. Wu, "Three-Dimensional Circular Patch Antenna Under TM02 Mode with Improved Impedance Matching," Electronics Letter, vol. 55, no. 4, pp. 169–170, 2019.

[9] S. Pyo, S. M. Han, J. W. Baik, and Y. S. Kim, "A Slot-Loaded Composite Right/Left-Handed Transmission Line for a Zeroth-Order Resonant Antenna with Improved Efficiency," IEEE Transaction on Microwave Theory and Techniques, vol. 57, no. 11, pp. 2775–2782, 2009.

[10] J. Tak and J. Choi, "Circular-Ring Patch Antenna with Higher Order Mode for On-Body Communications," Microwave Optical Technology Letters, vol. 56, no. 7, pp. 1511-1729, 2014.

[11] S. Gao, L. Ge, D. Zhang, and W. Qin, "Low-Profile Dual-Band Stacked Microstrip Monopolar Patch Antenna for WLAN and Car-to-Car Communications," IEEE Access, vol. 6, pp. 69575–69581, 2018.

[12] N. Nguyen-Trong, A. Piotrowski, T. Kaufmann, C. Fumeaux, "Low-Profile Wideband Monopolar UHF Antennas for Integration onto Vehicles and Helmets" IEEE Transactions on Antennas and Propagation, vol. 64, no. 6, pp. 2562–2568, 2016.

[13] S. Zhang, H. Zhang, B. Di, and L. Song, "Cellular UAV-to-X Communications: Design and Optimization for Multi-UAV Networks," IEEE Transactions on Wireless Communications, vol. 18, no. 2, pp. 1346–1359, 2019.

[14] Z. Liang, J. Liu, Y. Li, and Y. Long, "A Dual-Frequency Broadband Design of Coupled-Fed Stacked Microstrip Monopolar Patch Antenna for WLAN Applications," IEEE Antennas and Wireless Propagation Letters, vol. 15, pp. 1289 – 1292, 2016.